ORIGINAL ARTICLE

Research on typical soil physical properties in a mining area: Feasibility of three-dimensional ground penetrating radar detection

Gubai Luo[1] · Yingui Cao[1,2] · Hanxiao Xu[1] · Geng Yang[1] · Shufei Wang[1] · Yuhan Huang[1] · Zhongke Bai[1,2]

Abstract

The mining and reclaiming techniques of open-pit coal mines will affect the physical properties of the soil and the growth of vegetation. The traditional method of obtaining soil physical properties is time-consuming and laborious, so developing a rapid and non-destructive method for detecting typical soil physical properties in mining areas is of great significance for reclamation work. To study the typical soil physical properties of the reclaimed land in the mining area, we took the dumping sites of the Antaibao Open-pit Mine of China Coal as the research object and obtained measured data through the Ground Penetrating Radar (GPR) detection method and the soil profile sampling method. Then, the image analysis method, statistical analysis method and comparative analysis method were used to analyze the spatial variability for the soil moisture content, the effective soil layer thickness and the soil gravel content in the reclamation area. The results support the following conclusions: (1) The typical soil physical properties, namely, the soil moisture content, the effective soil layer thickness and the soil gravel content, of the reclaimed land in the mining area vary spatially. (2) Locally strong and fluctuating strong reflections in the 3D GPR image indicate that the detected sample is partially rich in water, and the spatial variability in the sudden moisture content of the reclamation in the mining area can be analyzed. (3) A low-frequency signal with good continuity in the 3D GPR image indicates that there is soil stratification under the detected sample, and the depth of the low-frequency signal with good continuity in the 3D GPR image can be used to characterize the effective soil layer in the reclaimed area. (4) The soil gravel content of the reclaimed soil can be analyzed from the statistics of the number of isolated gravel signals in the 3D GPR image. The greater the number of isolated gravel signals is, the higher the soil gravel content is. These conclusions, from both horizontal and vertical perspectives, suggest that 3D GPR images can be used to determine the typical physical properties of soil in a reclaimed land. These results can provide technical support for the efficient reclamation of a mining area and related restoration work.

Keywords Ground Penetrating Radar · Accurate reclamation · Soil moisture content · Effective soil layer thickness · Soil gravel content

Introduction

The BP World Energy Statistical Yearbook 2019 released by British Petroleum Corporation showed that global coal production exceeded 8 billion tons in 2018. China's coal production accounted for 46% of the world's total output. Coal has a considerable impact on the economic development of major coal countries. However, the problems of environmental pollution and ecological damage caused by coal mining are also becoming increasingly prominent. Coal mining can damage the land, cause geological disasters, threaten people's lives and property, and the disorderly stacking of coal gangue can pollute the soil and atmosphere, while mining wastewater will pollute the groundwater (Bian et al. 2010; Chabukdhara et al. 2016; Yang, 2019; Luo 2019). In addition, coal mining will lead to a series of land use limitations, decrease biodiversity, and impact human settlements (Cao et al. 2018). Land reclamation refers to taking measures to rectify the land that has been destroyed by production and construction activities and natural disasters. The reclamation

✉ Yingui Cao
  caoyingui1982@126.com

1 School of Land Science and Technology, China University of Geosciences, Beijing 100083, People's Republic of China

2 Key Laboratory of Land Consolidation and Rehabilitation, Ministry of Natural Resources, Beijing 100035, People's Republic of China

of damaged land in the mining area can effectively solve a series of ecological and environmental problems caused by coal mining and alleviate the limitation of land use in mining areas.

The restoration and reconstruction of the ecosystem in a mining area is mainly composed of five stages: landform reshaping, soil reconstruction, re-vegetation, landscape restoration and biodiversity reorganization and protection (Bai et al. 2018). Among them, soil reconstruction is the key to the restoration mining ecosystems. The quality of reconstructed soil is the main criterion for testing soil reconstitution (Hu et al. 2005). Soil profile rebuilding is the key to soil reconstruction. Soil profile rebuilding refers to the use of reasonable mining processes and reconstruction processes such as stripping, stacking, storage and back-filling to construct a soil physical environment suitable for soil profile development and vegetation growth. However, in the process of soil profile rebuilding, the soil stratification and structure often vary regionally and in vertical profile, these changes are manifested by typical soil physical properties impacted by mining, such as the difference in the soil moisture content, the effective soil layer thickness, the soil gravel content. The soil physical properties directly affect the soil fertility status, which in turn affects the growth of vegetation (Li et al. 2017). When domestic and foreign scholars evaluate the soil quality of reclaimed soil, the soil moisture content, the soil layer thickness, the soil gravel content and will be considered (Domínguez-Haydar et al. 2019; Hu et al. 2018; Luo et al. 2019). Soil water content directly affects vegetation growth and plant community diversity (Huang et al. 2004; Guo et al. 2005; Ersahin et al. 2006), so improving soil water storage and water holding capacity during land reclamation, and providing vegetation with the necessary moisture conditions are conducive to the restoration of vegetation in a mining area (Yu et al. 2016). Soil layer thickness affects soil microbial activity and soil fertility, which in turn affects vegetation growth (Meerveld et al. 2006; Chen 2016; Li et al. 2016). Soil gravel content mainly affects soil temperature and water characteristics (Cerda et al. 2001). Topsoil-covered gravel can reduce the rill flow rate and erosion rate (Wang et al. 2011). In addition, the presence of soil gravel also has a large impact on the content of various elements, such as carbon and nitrogen, and the solute transport process in soil (Certini et al. 2004). Therefore, it is of practical significance to study the soil moisture content, the soil layer thickness, the gravel content and as the typical physical properties of the reclaimed land in the mining area.

Traditional methods for measuring soil physical properties such as soil moisture content, soil layer thickness, and soil gravel content require digging the soil profile, which not only destroys the soil structure but also takes time and effort (Wang et al. 2016; He et al. 2009). With the rapid advancement of ecological civilization construction,

traditional measurement methods no longer meet normal production needs, so an efficient measurement method is urgently needed. In addition, there is a certain degree of degradation in the reclamation area of a mining area (Liu et al. 2017; Wang et al. 2020), so a rapid testing tool is needed to test the physical properties of the soil. As a new type of shallow geophysical detection technology, GPR is fast, convenient, and nondestructive, and produces continuous and, repeatable large-area measurements. A 3D GPR display can show the internal structure of an entire area at one time, and small structures that are easily missed or misjudged in a single profile can be easily displayed in 3D (Wang et al. 2007, 2018), which provides an accurate and effective means of detection for the reclamation of damaged land in mining areas. The application of GPR in soil evaluation is gradually expanding. The research of Benedetto (2010) shows that GPR can accurately measure soil water content and determine the change in water content in time and space. Wu et al (2014) used GPR to detect the soil moisture content of loam and sand. They pointed out that the accuracy of GPR in detecting soil moisture content is higher than that of time-domain reflectometry (TDR). Li et al (2014) used a 3D GPR model to analyze the distribution of soil water content in a seepage area, this approach provides a basis for using GPR to analyze the spatial distribution of soil moisture content in reclaimed land of mining areas. Studies have shown that GPR can be used to detect complex geological structures and rock thickness, and provides good agreement with the results obtained by traditional survey methods, but certain errors arise (Yang et al. 2014; Yu et al. 2011). Brosten et al (2009) used GPR to study the dependence of thawing depth on channel morphology. Studies have shown that GPR detection can provide a detailed 3D geometry of the active layer melting depth, this approach provides a basis for using GPR to investigate the effective soil layer thickness geometry of the reclaimed land in the mining area with the support of 3D data. GPR has been less frequently applied in the detection of soil debris, and has only been evaluated from the perspective of experimental analysis, but its application has been proven (Eriksson 1996; He et al. 2009). Anchuela et al. (2019) used GPR to evaluate the scale of heterogeneous bodies at different scales and the discontinuities caused by the existence of voids in rocks. The research of Zenone et al (2008) shows that the resolution of GPR increases with increasing antenna frequency. The higher the frequency is, the more particles with a smaller diameter can be distinguished, which provides a basis for high-frequency GPR to detect surface soil gravel content. In the current literature, few studies have been presented on the typical soil physical properties of reclaimed land in coal mining areas, especially 3D exploration based on GPR to investigate the typical soil

physical properties of a mining area. Therefore, we took the dump sites of the Antaibao Open-pit Mine of China Coal as the research object, and used the new shallow geophysical detection technology (GPR technology) to realize the rapid, nondestructive probing of typical soil physical properties in the mining area, in particular, the 3D model was used to examine the internal structure of the soil in the whole reclamation area, which provides more favorable support for the reclamation of damaged land.

Materials and methods

Research area overview

The study area is located Antaibao Open-pit Mine in the Pingshuo, China Coal in Pinglu District, Shuozhou City, Shanxi Province (Fig. 1). It is located in the Black Triangle of the border between Shanxi, Inner Mongolia and Shannxi in the Loess Plateau. In the zone, the coal geological reserve is approximately 12.70 billion tons. The Antaibao Open-pit Mine, where the study area is located, is located at 112°11′-113°30′ east longitude and 39°23′-39°37′N′ north latitude. It has a temperate semiarid continental climate with strong winds in winter and spring. The average annual number of winds above 8 is over 35 days, up to 47 days, which makes the soil physical weathering strong. The annual average temperature is 4.8–7.8 °C, the annual precipitation is only approximately 450 mm, and is mainly concentrated in July, August and September. The evaporation is approximately 5 times the annual precipitation, which makes the soil in the mining area dry and water-poor, prone to flood disasters and soil erosion. The soil type in the mining area is the transition type of chestnut soil and chestnut-cinnamon soil. The soil is sandy and has a poor water retention capacity. This has limited the

restoration of the ecosystem in the mining area and made the ecological environment fragile.

Data sources and test

To study the spatial distribution of the soil moisture content, the effective soil layer thickness and the soil gravel content of reclamation areas, nine plots were established in different areas of the South Dumping Site, West Dumping Site and Internal Dumping Site (Fig. 1). A soil profile with length, width and height of 1.20 m × 1 m × 1 m was excavated in the sample plot, and a soil ring knife sample was collected every 10 cm in the profile.

$$\theta_v = \frac{m_{wet} - m_{dry}}{v} \tag{1}$$

In formula (1): θ_v is the soil moisture content; m_{wet} and m_{dry} are the soil wet weight and soil dry weight, respectively, g; v is the volume of the ring cutter, 100 cm³, and the density of water is assumed to be 1 g/cm³.

The soil profile was observed, the number of gravel particles in the depth range of 0–40 cm was counted, and the effective soil thickness of the profile was recorded.

GPR detection

In the test area of the dumping site, a 1 m × 1 m sampling plot was established, and a line with a spacing of 10 cm was arranged in the sampling plot. The GPR was used to detect along the line direction (Fig. 2) to obtain an image of the soil profile and detect the spatial variability in the characterizing the soil moisture content and the effective soil layer
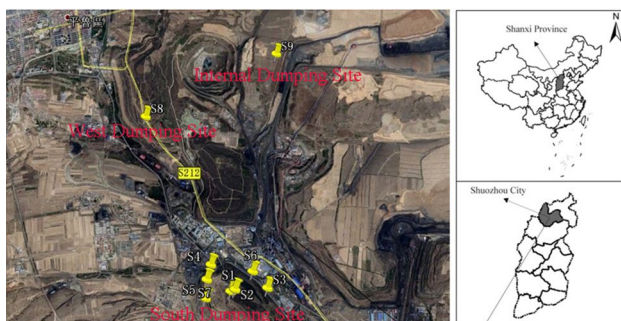
Dumping sites of Antaibao Open-pit Mine, China Coal

Fig. 1 Dumping sites and sampling plots in Antaibao Open-pit Mine, China Coal

Fig. 2 Detection process with GPR

thickness. Two lengths of 2 m lines were selected near each plot, and GPR was used along the line. The acquired images were used to study the changes in the soil gravel content in the reclaimed surface of the mining area. During the detection process, according to the actual conditions, an antenna with the appropriate frequency was selected to detect the typical soil physical properties of the reclaimed land in the mining area. We selected an antenna with a frequency of 900 MHz and a detection depth of approximately 1 m. Before detection, the electromagnetic wave velocity was set to 0.10 m/ns in the radar host, the dielectric constant was 8 (8 is the empirical dielectric constant of the soil), and the time window was 25 ns. To avoid the impact of concentrated rainfall on the test results, when using GPR to detect the soil moisture content, our tests were conducted in May 2018 and May 2019, during non-rainy seasons.

GPR detection image processing

After obtaining the detection images of each profile, each image was processed by IDSP7.0 software, via zero-point adjustment, one-dimensional filtering, interchannel equalization, background elimination, wavelet denoising, etc. The zero-point adjustment was used to move the radar profile image up and down and identify the interface between the atmosphere and the ground so that only the underground part of the image was considered. The role of one-dimensional filtering was mainly to suppress the interference signal to improve the signal-to-noise ratio and extract the response characteristic signal of the underground medium. The interchannel equalization enhanced the signal through the correlation between the channels. For the uncorrelated signals between the channels, the processed signal was weakened. This method greatly enhanced the weak signals with good correlation in the radar profile image. Background elimination highlighted abnormal signals, eliminated background noise and standing wave interference due to impedance

mismatch, compressed horizontal interference signals and extracts useful signals. Wavelet denoising was also used to suppress noise signals and boost useful signals. After the basic processing of the detected image, the data of the different lines were synthesized into 3D data to form a 3D slice, and finally, a 3D image was formed.

Results and analysis

Profile characteristics of soil physical properties

The soil moisture content, the amount of gravel and the thickness of the soil layer of each soil profile were obtained by indoor and outdoor experiments, as shown in Table 1. Because of the large amount of gravel, the soil moisture content of P_3 was only measured for the 0–10 cm and 10–20 cm soil layers. Table 1 shows that the soil moisture content at P_1 at 10–20 cm is 33.90%, much larger than that at the other soil layers. The soil moisture content of P_2 at 0–20 cm is greater than the soil moisture content at 20–40 cm. The moisture content of the soil of P_4 at 0–40 cm is less than or equal to 40 cm. The moisture content of soil at 0–10 cm in P_5, P_8 and P_9 is less than 10 cm, and the soil moisture content of the soil layers in P_6 and P_7 does not change much. P_2 and P_3 have more gravel content, 21 and 22 gravel particles, respectively. The surface soil has a large gravel content, followed by P_5 and P_7, which have 14 and 11 gravel particles, respectively. The surface soil has a small gravel content. P_6 contains 6 gravel particles, and the gravel content is very small. P_1, P_4, P_8, and P_9 do not exhibit gravel particles, and the soil profile is a homogeneous profile. P_2, P_4, P_5 and P_6 exhibit obvious stratification, and the thickness of the soil layer is greater than 20 cm.

Table 1 Characteristics of soil physical properties in each profile

Profile properties		P_1	P_2	P_3	P_4	P_5	P_6	P_7	P_8	P_9
Soil moisture content (%)	0–10 cm	8.70	17.10	24.10	23.70	15.80	26.80	14.30	12.87	12.18
	10–20 cm	33.90	22.10	20.00	27.30	24.20	27.90	13.20	16.84	18.39
	20–30 cm	9.30	13.90		31.30	21.20	31.90	14.60	15.17	21.56
	30–40 cm	15.20	15.30		20.60	28.90	35.50	15.60	16.38	23.68
	40–50 cm	11.20	13.40		15.30	29.40	34.50	14.30	18.42	24.38
	50–60 cm	13.60	21.90		14.90	28.40	18.40	17.80	15.37	18.56
Number of gravel particles		0	21	22	0	14	5	11	0	0
Soil thickness (cm)		>100	29	3	26	10	49	>100	>100	>100

Note: Because the soil gravel content below 20 cm is relatively large, the soil cannot be sampled under 20 cm in P_3 profile, so there are no soil moisture content data of 20–60 cm. P_5 is a soil-rock mixed profile. The soil gravel content in P_7 is low, mainly soil. P_1, P_8 and P_9 are pure soil profiles. P_2, P_4 and P_6 have obvious soil and coal gangue stratification

3D image characteristics for soil moisture content change

Four soil profiles with different soil moisture contents along the depth direction were selected from the previous nine profiles, and a 3D GPR image of detection was obtained, as shown in Fig. 3. On the whole, similar to the measured results of the digging soil profile method, the soil moisture content varies in space. The low-frequency signal of P_1 is low at 0–10 cm, and there is no local strong reflection, indicating that the soil moisture content of P_1 is relatively low at 0–10 cm. Both strong and weak changes are observed at 10–40 cm, and the signal intensity of the local reflection is strong, indicating that the soil moisture content at this depth is large. P_2 exhibits strong and weak changes at 0–20 cm and 50–60 cm, and the signal intensity of local reflection are strong, indicating that the soil moisture content at these two depths is greater than the soil moisture content at other depths. P_8 and P_9 have fewer low-frequency signals at 0–10 cm, and no local strong emission occurs, indicating that the soil moisture contents of P_8 and P_9 are relatively low at 0–10 cm.

Comparing the measured soil moisture content of each profile in Table 1, the spatial variability of the soil moisture content characterized by the 3D image around P_2, P_8 and P_9 are similar to the measured results, but the soil moisture content information of the soil layer below 10 cm characterized by the 3D image of P_1 are not exactly the same as the measured values. It is feasible to characterize the soil moisture content of reclaimed land in mining areas by 3D GPR images.

3D image characteristics for effective soil layer thickness

Three soil profiles with typical stratification were selected from the nine plots, and the 3D image of the GPR detection are shown in Fig. 4. It can be seen from the figures that the soil profile with typical stratification also has obvious stratification signals in the 3D image obtained by GPR detection, among them, the stratification signal of P_2 is between 30 and 40 cm, which of P_4 is between 20 and 30 cm, and that of profile P_6 is between 30 and 40 cm.

The thickness of the effective soil layer obtained by excavating the soil profile was 29 cm for P_2, 26 cm for P_4, and 49 cm for P_6, as shown in Table 1. By comparing the depth of the measured soil profile with the depth of the stratification signal in the 3D GPR images, only the measured depth of P_4 is within the range of the stratification signal of the 3D image. The measured depths of P_2 and P_6 are both greater than the range of the 3D image stratification signal. Thus, the depth of the soil detected by the GPR is not necessarily the true depth. To detect the true thickness of the soil layer, the true dielectric constant corresponding to this soil layer must be obtained.

Observing the 3D images of the three profiles, the x-direction and the y-direction both exhibit obvious stratification, the continuity of the stratification in both directions is good, and the stratifications in the two directions correspond well, indicating that the GPR can be used to check the soil stratification of reclaimed land in a mining area.

3D image characteristics for soil gravel content

The isolated debris signal in the GPR image is delineated in the manner shown in Fig. 5, and the number of isolated gravel signals along each line is counted as shown in Table 2. It can be seen from Table 2 that there are some differences in the number of isolated gravel signals in different profiles of the GPR images, indicating that there is a certain variability in the degree of gravel content in the soil. On the whole, when the line length is 1 m, the number of signals of isolated gravel in P_2, P_3, P_5 and P_7 of the GPR images are relatively large, all of which are greater than 8. This is the same as the results from the soil excavation profiles in Table 1, which indicates that GPR can be used to detect the gravel content of the surface soil of the reclaimed land in a mining area.

Comparing the results in Table 1 and Table 2, when the length of the survey line is 1 m, the number of gravel particles in P_2, P_3, P_5 and P_7 obtained by the excavation of the soil profile method are greater than that obtained by the GPR detection method, which is related to the antenna used in GPR detection and the burial depth of isolated gravel in the soil. The larger the frequency of the antenna is, the smaller the diameter of the isolated body in the soil that can be detected. The deeper the burial depth of the isolated gravel in the soil is, the more difficult it is to detect by GPR.

According to the statistics of the soil profile method, the number of gravel particles in P_2, P_3, P_5 and P_7 (pure soil profiles) are 0. However, there are also a certain number of isolated gravel signals in the GPR images, which indicates that in addition to potential isolated gravel particles, there may also be isolated heterogeneous bodies that are electrically different from the soil. This finding also relates to the movement of the antenna during the detection process. On the whole, it is feasible to quantitatively analyze the soil gravel content of the reclaimed soil in the mining area using GPR-detected images (Fig. 6).
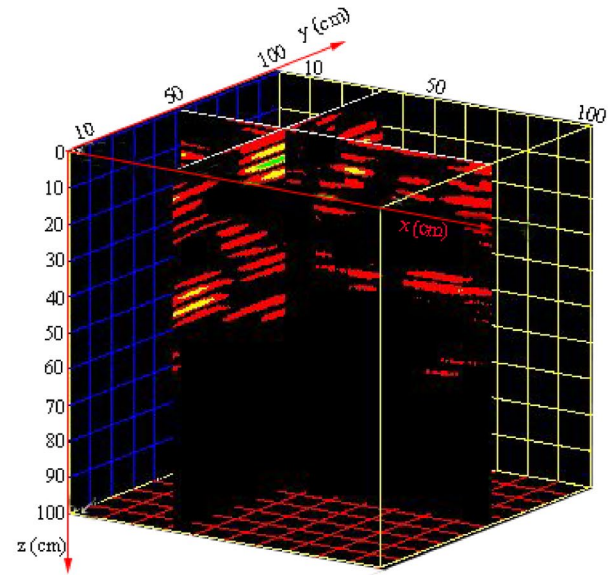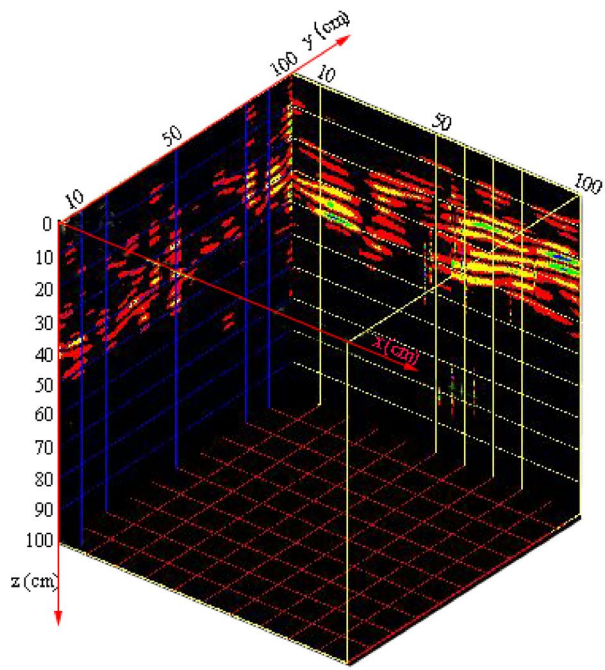
P$_1$

P$_2$
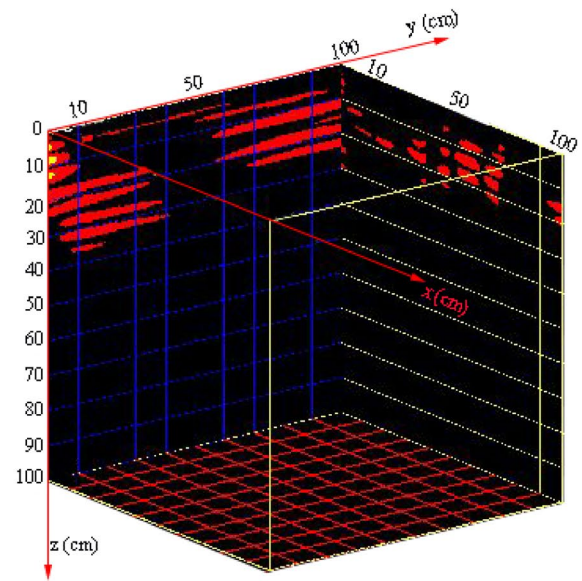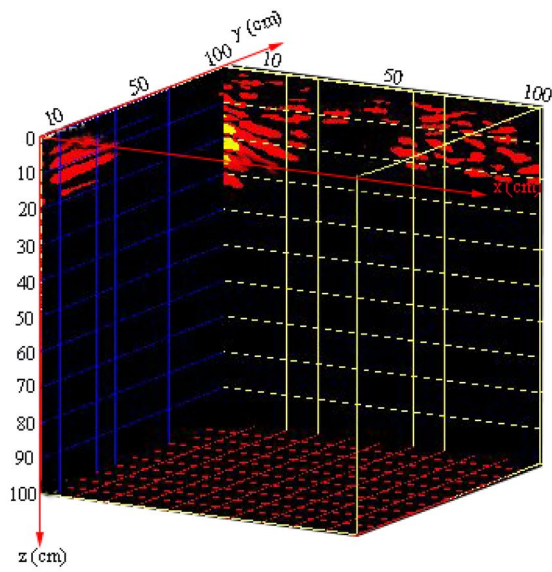
P$_3$

P$_4$

Fig. 3 Soil moisture content of detection images

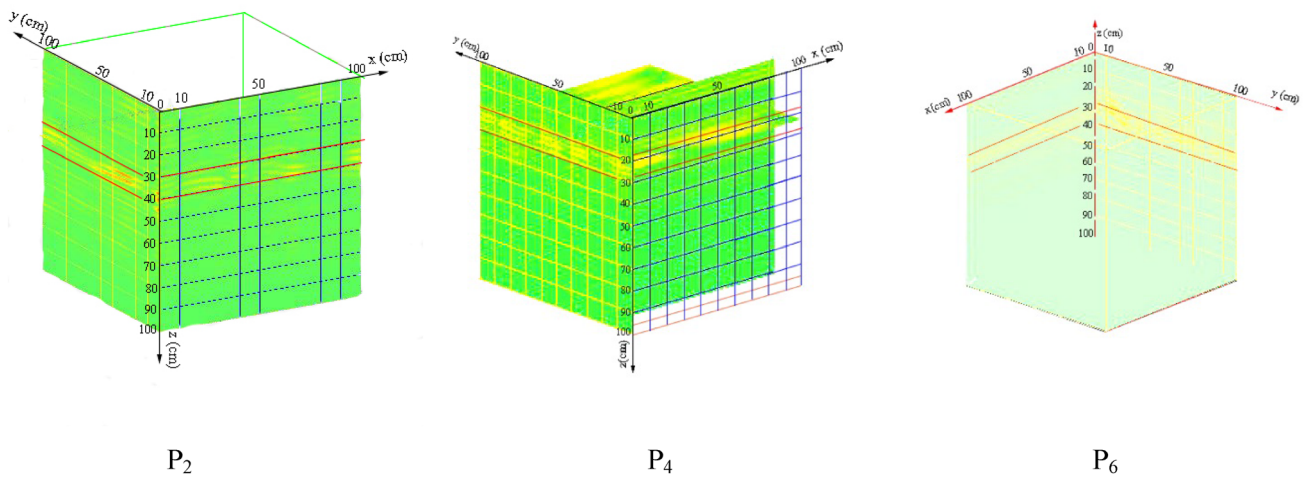P_2 P_4 P_6

Fig. 4 Effective soil layer thickness of detection images. The 3D images of the soil profile processed by IDSP7.0 software do not directly display depth on the coordinate axis. In the 3D images, each small plot is 10×10 cm and can be used to estimate the depth of the stratification signal in the 3D image of the soil profile
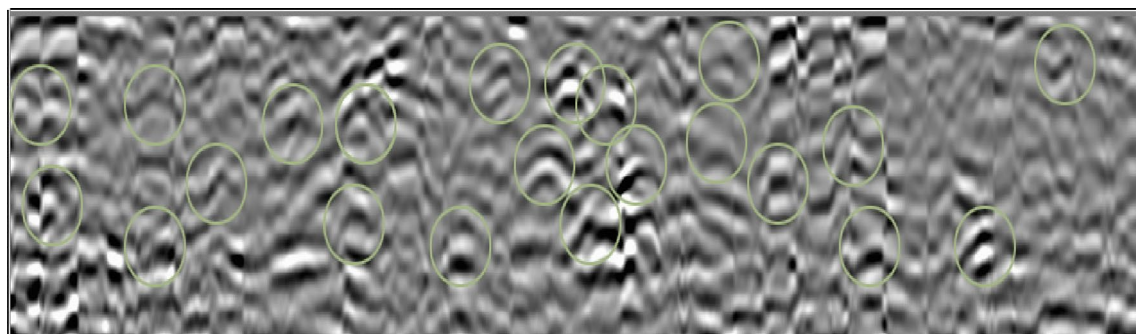

Fig. 5 Soil gravel signals in the GPR image

Discussion

3D GPR characterization of changes in the soil moisture content

A 3D GPR image can be used to analyze the spatial variation in soil moisture content in a typical area. Influenced by soil dumping and land making techniques, the soil moisture content of the reclaimed land in a mining area is varied spatially (Liu et al. 2019). The dielectric constant represents the ability of a dielectric to bind charges. Dry sand has a dielectric constant between 4 and 10, and freshwater has a dielectric constant of 81. The greater the moisture content in the soil is, the greater of the dielectric constant is and the stronger of the ability is to bind the charge. When electromagnetic waves propagate in soil, the electromagnetic waves are strongly absorbed and strongly reflected at the interface where the soil moisture content differs greatly. In 3D GPR images, the intensity of the low-frequency signal is variable, and the local reflection is strong (Buchner et al. 2010). Therefore, in theory, the spatial variation in soil moisture content in reclaimed land in mining areas can be analyzed by 3D GPR images.

Ocaña-Levario et al. (2018) analyzed the water leakage of a water supply system (WSS) by using a 3D image after GPR detection and processing based on the difference in the dielectric constant of three different media, namely, the pipeline, water and soil. They thought of that with the help of GPR images, the abnormal characteristics of the pipeline can be displayed intuitively. As a kind of dispersive medium, the water-rich soil has a slower propagation speed and faster attenuation than a nondispersive medium, and it is characterized by the presence of a difference and continuous reflection in GPR images, which matches the research results of Yang et al. (2014) and other researchers who used GPR to detect a water-rich fractured sandstone area. These previous studies have shown that GPR can be used for analysis as long

Table 2 Gravel signal statistics in different profiles

Profiles	Survey line	Number of gravel signals	Total	Converted to 1 m line
P_1	L01	8	14	3
	L02	6		
P_2	L03	16	32	8
	L04	16		
P_3	L05	18	40	10
	L06	22		
P_4	L07	16	24	6
	L08	8		
P_5	L09	14	32	8
	L10	18		
P_6	L11	10	21	5
	L12	11		
P_7	L13	16	32	8
	L14	17		
P_8	L15	7	14	3
	L16	7		
P_9	L17	9	19	5
	L18	10		

as there is a certain difference in dielectric constant among the media. This conclusion is similar to the results of this paper using 3D GPR images to analyze the spatial variation in soil moisture content in reclaimed land of mining areas.

3D image characterization to determine the effective soil layer thickness

A 3D GPR image can be used to analyze the variation in the soil thickness in space, which is a typical soil physical property. Affected by the excavation and land-making process and benefit-driven decisions, when the damaged land is reclaimed, the topsoil cover is often thin, and the coal gangue may even be exposed, as shown in Fig. 6. This will have a certain impact on the growth of vegetation after reclamation. Effective soil layer thickness refers to the topsoil thickness required for vegetation growth. Coal gangue and topsoil are two different media (Yang et al. 2007; Fan et al. 2010), and the dielectric constants of the two media are different. When electromagnetic waves propagate to the interface between the coal gangue layer and the topsoil layer, strong emission occurs, and because the stratification of coal gangue and topsoil is generally continuous, this is characterized by continuous low-frequency signals and a large phase difference in the 3D GPR image (Leandro et al. 2019). Therefore, in theory, the 3D GPR image can be used to analyze the spatial variation in the effective soil layer thickness in the reclamation area of mining areas.

Chen et al (2015) used GPR to detect seawalls and accurately identified defect information and layered information in GPR detection images. The target body they detected is the defect in the seawall, which is different from the surrounding medium in electrical properties and has a certain scale, which is similar to the condition of using GPR images to analyze the effective soil thickness of the reclaimed land in the mining area. Han et al (2016) and Hu et al (2005) and others used GPR to detect soil layered structures. They suggested that GPR can effectively determine the thickness of soil layers but did not provide a method to determine the depth of stratification. Roth et al (2004) and others have shown that GPR can be used for the exploration of soil layers and shallow groundwater surfaces. Seyfried et al. (2016) used GPR to determine the optimum height for cutting soil. Previous studies have shown that GPR can be used

Fig. 6 Topsoil of the reclaimed land in the mining area

to analyze the layered information of the medium, which is similar to the GPR image used in this paper to analyze the spatial variation in the effective soil layer thickness in the mining area.

Analysis of the soil gravel content with 3D image characterization

By counting the number of isolated gravel signals in the GPR image, the gravel content of the reclaimed surface soil in the mining area can be analyzed. Affected by the method of reclamation, there are gravel particles at different depths of the reclaimed land in the mining area. The size of these gravel particles will affect the quality of the soil and affect the growth of the vegetation. Isolated gravel particles and its surrounding soil are two different media, and there are certain electrical differences. Electromagnetic waves will be reflected at the interface between gravel and soil and appear as a black and white signal features in a GPR image (Qian et al. 2004). The GPR transmitting antenna transmits spherical waves to the ground (Wang and Wu, 2010), so the signal of an isolated gravel particle in the image is a parabola with a downward opening. The greater the number of parabolas is, the greater the number of isolated gravel particles is in the soil, and the higher the gravel content of the surface soil. Therefore, it is theoretically feasible to analyze the gravel content of the surface soil by counting the number of signals of such isolated gravel particles.

Anchuela et al. (2019) and Berton et al (2019) argue that the larger the antenna frequency, the easier it is to identify small-diameter bodies in the medium. Shakas et al. (2017) used GPR to analyze the spatial distribution of fractures in rocks. Yamase et al (2018) used GPR to analyze the spatial distribution of vegetation roots in the soil. Previous studies have fully demonstrated that GPR can be used to analyze the spatial distribution characteristics of isolated solids in a medium, which is similar to the analysis of isolated gravel particles in the reclaimed surface layer of a mining area. Thus, the soil gravel content in the reclaimed surface layer of a mining area can be determined by interpreting GPR imagery.

Application and deficiency

Soil moisture content

By analyzing 3D GPR imagery of the reclaimed land, the process of re-vegetation in the damaged area of the mining area can be determined to identify the infiltration depth after watering and determine the optimum watering amount, promote vegetation growth and accelerate the process of vegetation restoration. At the same time, the infiltration depth after

rainfall can be detected, and the soil voids can be analyzed. This approach can be used to reveal the spatial distribution of the soil moisture content. In this paper, there are still some deficiencies in the study of soil moisture content. If the soil moisture content is not high in a certain area, or the difference in soil moisture content between different layers in the soil is small, and the reflection information in the GPR image is weak (Luo et al. 2019). It is impossible to analyze the soil moisture content from a 3D GPR image. Generally, the key to solving this problem is to improve the GPR data processing technology and use a higher frequency antenna in GPR detection.

Effective soil layer thickness

From the 3D GPR image of the reclaimed land, the spatial variability in of effective soil layer thickness can be analyzed. In the process of repairing the damaged land in the mining area, the spatial change in the topsoil in the process of soil reconstruction can be detected to ensure that the requirements of the covering soil thickness in the Quality Control Standard for Land Reclamation are met. At the same time, examining the spatial distribution of the thickness of the degraded reclaimed soil layer provides the basis for analyzing the thickness of the reclaimed land for re-vegetation. In this study, 3D GPR images were used to analyze the spatial variation in effective soil layer thickness, but the effective soil layer thickness was not accurately determined. To accurately determine the effective soil layer thickness and quantitatively detect the accuracy of the thickness of the reclaimed soil in the mining area, a more accurate dielectric constant is needed (Xu et al. 2000).

Soil gravel content

By counting the number of isolated gravel signals in the GPR image, the gravel content of the surface soil in a reclamation waste dump can be analyzed, and the gravel content of the surface soil can be provided to the department of reclamation soil quality supervision. The number of isolated gravel signals in GPR images can be used to provide researchers with an index of soil gravel content analyze vegetation growth and predict the possibility of soil erosion. There are some inadequacies in the study of the surface gravel content of the reclaimed land in this mining area. In this study, two 2 m-long lines were used to represent the whole sample with only a few measuring lines, but the number of lines and the length of lines could be increased. Affected by the antenna frequency, large gravel particles distributed deep in the soil could not be identified, and some small-diameter and widely distributed isolated solids could not be identified (Wang et al. 2009).

In general, the 3D display of GPR can be used to investigate the spatial changes in soil physical properties such as the soil moisture content, the soil thickness, and the

soil gravel content. However, using GPR to investigate the internal structure of reconstructed soil and detect whether it can achieve quality standards requires the use of more measuring lines, and the cost will increase. In addition, to accurately detect the thickness of the soil layer, it is necessary to determine the exact dielectric constant.

Conclusions

In this paper, the new GPR detection technology is used to detect the reclaimed dumping sites of the Antaibao Open-pit Coal Mine in Pingshuo, Shanxi Province, and 3D images of the soil are analyzed. Through the method of digging the soil profiles, the basic characteristics of the typical soil physical properties of the reclaimed land in the mining area are obtained. By comparing the typical physical properties of the mining area soil obtained by the profile method and the GPR detection method, the typical soil physical properties of the reclamation land based on 3D GPR images are validated, and the feasibility of applying this technology to the efficient reclamation of a mining area and related restoration work is proven.

(1) A 3D GPR image can be used to analyze the spatial variation in soil moisture content. If there is strong weak fluctuating strong reflection in a local part of the 3D GPR image, the detected sample is partially rich in water, and the sudden spatial variability of the soil moisture content can be analyzed.

(2) The 3D GPR image can be used to analyze the variation in the effective soil layer thickness. A low-frequency signal with good continuity in the 3D GPR image indicates that there is soil stratification under the detected sample, and the depth of the low-frequency signal with good continuity in the 3D GPR image can represent the depth of the effective soil layer thickness.

(3) By counting the number of isolated gravel signals in the GPR image, the soil gravel content of the reclaimed surface soil in the mining area can be analyzed. The more isolated the gravel signal is in the GPR image, the higher the gravel content is in the reclaimed surface soil.

These three conclusions suggest that 3D GPR images can be used to determine the typical physical properties of soils in a certain area of mining reclamation, and with reference to other influencing factors, the appropriate vegetation planting patterns in the area can be determined. This technology can provide technical support for the efficient reclamation of a mining area and related restoration work.

Compliance with ethical standards

References

Anchuela OP, Luzon A, Perez A et al (2016) GPR evaluation of the internal structure of fluvial tufa deposits (Dévanos-Añavieja system, NE Spain): an approach to different scales of heterogeneity. Geophys J Int 206(1):557–573

Bai ZK, Zhou W, Wang JM et al (2018) Re-discussion on restoration and reconstruction of mining ecosystem. China Land Sci 32(11):1–9

Benedetto A (2010) Water content evaluation in unsaturated soil using GPR signal analysis in the frequency domain. J Appl Geophys 71(1):26–35

Berton F, Guedes CC, Vesely FF et al (2019) Quaternary coastal plains as reservoir analogs: Wave-dominated sand-body heterogeneity from outcrop and Ground Penetrating Radar, central Santos Basin, southeast Brazil. Sediment Geol 379(1):97–113

Bian ZF, Inyang HI, Daniels JL et al (2010) Environmental issues from coal mining and their solutions. Min Sci Technol (China) 20(2):215–223

Brosten TR, Bradford JH, Mcnamara JP et al (2009) Estimating 3D variation in active-layer thickness beneath arctic streams using ground-penetrating radar. J Hydrol 373(3):479–486

Buchner JS, Wollschläger U, Schneider S et al (2010) Determining the influence of soil water content variability on GPR measurements with numerical simulations. Geophys Res Abstr 10:16–34

Cao YG, Dallimer M, Stringer L et al (2018) Land expropriation compensation among multiple interests in a mining area: Explaining "skeleton house" compensation. Land Use Pol 74:97–110

Cerda A (2001) Effects of rock fragment cover on soil infiltration, inter rill runoff and erosion. Eur J Soil Sci 52(1):59–68

Certini G, Campbell CD, Edwards AC (2004) Rock fragments in soil support a different microbial community from the fine earth. Soil Biol Biochem 36(2):1119–1128

Chabukdhara M, Singh OP (2016) Coal mining in northeast India: an overview of environmental issues and treatment approaches. Internat J Coal Sci Technol 3(2):87–96

Chen J, Ge SC, Zhao YH et al (2015) Wavelet processing and interpretation of radar detection image of seawall hidden danger. Chin J Undergr Space Eng 11(S1):337–341

Chen XY, Wang F, Yan JP et al (2016) Effects of soil thickness on day and night changes of reclaimed soil respiration in mining area. J China Univ Min Technol 45(1):163–169

Domínguez-Haydar Y, Velásquez E, Carmona J et al (2019) Evaluation of reclamation success in an open-pit coal mine using integrated soil physical, chemical and biological quality indicators. Ecol Indic 103:182–193

Eriksson CP, Holmgren P (1996) Estimating stone and boulder content in forest soils-evaluating the potential of surface penetration methods. CATENA 28(2):121–134

Ersahin S, Brohi AR (2006) Spatial variation of soil water content in topsoil and subsoil of a Typic Ustifluvent. Agric Water Manage 83(1/2):79–86

Fan WH, Li HF, Bai ZK et al (2010) Effects of coal gangue spontaneous combustion on reclaimed soil quality in large open pit mines in the Loess Plateau. Trans Chin Soc Agric Eng 26(2):319–324

Guo YY, Zhang JY, Gong HL et al (2005) Diversity of vegetation restoration process in reclaimed land in Antaibao mining area. Chin J Ecol 25(4):763–770

Han XL, Liu JT, Zhang J et al (2016) Identifying soil structure along headwater hillslopes using GPR based technique. J Mt Sci 13(3):405–415

He RZ, Hu ZQ, Wang J et al (2009) Research progress in detecting soil quality using ground penetrating radar. Prog Geophys 24(4):1483–1492

Hu ZQ, Wei ZY, Qin P (2005) Concept and method of soil reconstruction in mine reclamation. Soils 1:8–12

Hu ZQ, Duo LH, Shao F et al (2018) Optimal thickness of soil cover for reclaiming subsided land with Yellow River sediments. Sustainability 10:3853

Huang YZ, Zhu YG, Tong YP et al (2004) Effects of soil moisture on the uptake and accumulation of cadmium in maize seedlings. Chin J Ecol 24(12):2832–2836

Leandro CG, Barboza EG, Caron F et al (2019) GPR trace analysis for coastal depositional environments of southern Brazil. J Appl Geophys 162(5):1–12

Li J, Zeng Z, Chen L et al (2014) Estimation of mixed soil water content by impedance inversion of GPR data. *15th International Conference on Ground Penetrating Radar*.

Li Y, Shang SY, Liu ZX (2016) Correlation between the coverage of typical steppe vegetation and the spatial heterogeneity of chestnut soil thickness in Deligor. Jiangsu Agric Scis 44(11):411–418

Li HT, Zhang Y, Wei ZC et al (2017) Analysis of soil fertility of Chinese Fir plantation at different development stages. For Res 30(2):322–328

Liu XY, Cao YG, Bao ZK et al (2017) Evaluating relationships between soil chemical properties and vegetation cover at different slope aspects in a reclaimed dump. Environ Earth Sci 76:805

Liu BY, Li YY, Liu XL et al (2013) Study on microclimate effects of different reclamation modes in the discharge field of Haizhou Open-pit Mine. Earth Environ 47(1):88–96

Luo QW (2019) Analysis of the influence of coal mining on ecological environment and protection. Resour Inf Eng 34(1):85–86

Luo GB, Cao YG, Bai ZK et al (2019) Characterization and inversion of volumetric water content of reconstituted soil in loess open pit mining area. J Ecol Rural Environ 35(4):529–537

Meerveld HJT, Mcdonnell JJ (2006) On the interrelations between topography, soil depth, soil moisture, transpiration rates and species distribution at the hillslope scale. Adv Water Resour 29(2):293–310

Ocaña-Levario SJ, Carreño-Alvarado EP, Ayala-Cabrera D et al (2018) GPR image analysis to locate water leaks from buried pipes by applying variance filters. J Appl Geophys 152:236–247

Qian RY, Wang ZC, Kong XC et al (2004) Application of ground penetrating radar to nonmetallic pipeline detection. Munic Technol 22(5):327–329

Roth K, Wollschlager U, Cheng ZH et al (2004) Exploring soil layers and water tables with ground penetrating radar. Pedosphere 14(3):273–282

Seyfried D, Schoebel J (2016) Ground Penetrating radar for asparagus detection. J Appl Geophys 126:191–197

Shakas A, Linde N (2017) Apparent apertures from GPR data and their relation to heterogeneous aperture fields. Geophys J Int 209(3):1418–1430

Wang ZC, Wu W (2010) Geological radar technology for nondestructive testing of tunnel quality. Railw Technol Innov 3:78–80

Wang BB, Sun B, Tian G et al (2007) Analysis of sea ice thickness and surface morphological characteristics of Arctic summer using three-dimensional GPR. Geophys Geochem Explor 31(3):189–192

Wang M, Guo XJ, Luo H et al (2009) Detecting on pouring defects of large-scale concrete pipe and box culvert with GPR method. South-to-North Water Transf Water Sci Technol 7(6):211–215

Wang XY, Li CX, Xu QX et al (2011) Research progress of gravel coverage on soil water erosion process. China J Soil Water Conserv 9(1):115–120

Wang P, Hu ZQ, Zhao YL et al (2016) Experimental study of soil compaction effects on GPR signals. J Appl Geophys 126:128–137

Wang HH, Gong JB, Wang ML et al (2018) Application of 3D ground penetrating radar technology in road collapse cavity detection. CT Theory Appl Res 27(5):61–68

Wang SF, Cao YG, Pietrzykowski M et al (2020) Spatial distribution of soil bulk density and its relationship with slope and vegetation allocation model in rehabilitation of dumping site in loess open-pit mine area. Environ Monit Assess 192:740

Wu YB, Cui F, Wang L et al (2014) Detection of soil moisture content by transmissive ground penetrating radar. Trans Chin Soc Agric Eng 30(17):125–131

Xu SC, Liu F (2000) Research and application of ground penetrating radar in urban road thickness detection. J East China Jiaotong Univ 17(4):27–31

Yamase K, Tanikawa T, Dannoura M et al (2018) Ground Penetrating Radar estimates of tree root diameter and distribution under field conditions. Trees-Struct Funct 32(6):1657–1668

Yang XH (2019) Analysis of the impact of coal mining on the environment and its countermeasures. Technol Econ Guide 27(1):128

Yang ZQ, Hu ZQ, Wang JY et al (2007) Restoration ecology of coal gangue mountain reclamation. China Soil Water Conserv 6:35–36

Yang ZZ, Liu DW, Zhai FJ et al (2014) Study on signal characteristics of ground penetrating radar in water-rich fractured rock mass. J Wuhan Univ Technol 36(11):103–108

Yu XX, Ma XW, Di LX et al (2011) Experimental study of ground penetrating radar in soil thickness investigation. Acta Pedol Sin 48(4):874–878

Yu YJ, Ren SS, Guo LK et al (2016) Study on soil water storage characteristics of two types of reconstructed coal mines. Soil Water Conserv Res 23(2):44–48

Zenone T, Morelli G, Teobaldelli M et al (2008) Preliminary use of ground penetrating radar and electrical resistivity tomography to study tree roots in pine forests and poplar plantations. Funct Plant Biol 35(10):1047